AD-A021 468

INVESTIGATIONS INTO THE FEASIBILITY OF HIGH POWER LASER WINDOW MATERIALS

Jacob L. Zar

Avco Everett Research Laboratory, Incorporated

Prepared for:

Air Force Cambridge Research Laboratories

15 October 1975

DISTRIBUTED BY:

NTIS

National Technical Information Service
U. S. DEPARTMENT OF COMMERCE

FOREWORD

ARPA Order No: 2806

Program Code No: 5010

Name of Contractor: AERL, Inc.

Effective Date of Contract: 1-10-74

Contract No: F19628-75-C-0066

Principal Investigator and Phone No: Dr. J. L. Zar
(617) 389-3000, Ext. 225

AFCRL Project Scientist and Phone No: Drs. Rudolf Bradbury
and William E. Ewing
(617) 861-4922

Contract Expiration Date: 12-31-76

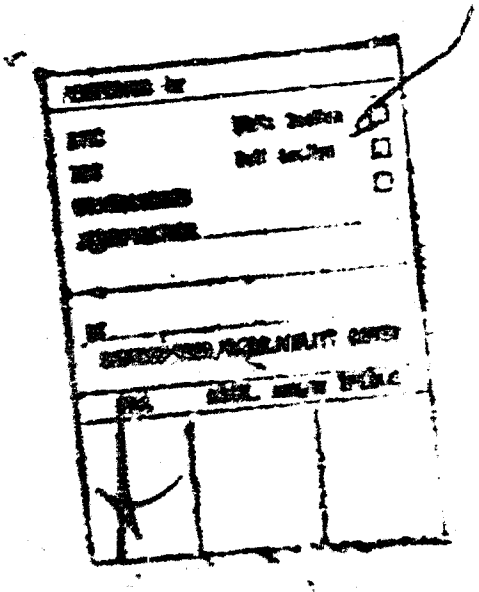

Qualified requestors may obtain additional copies from the Defense Documentation Center. All others should apply to the National Technical Information Service.

Best Available Copy

Unclassified

SECURITY CLASSIFICATION OF THIS PAGE (When Data Entered)

REPORT DOCUMENTATION PAGE	READ INSTRUCTIONS BEFORE COMPLETING FORM
1. REPORT NUMBER: AFCRL-TR-75-0605	2. GOVT ACCESSION NO. / 3. RECIPIENT'S CATALOG NUMBER
4. TITLE (and Subtitle): INVESTIGATIONS INTO THE FEASIBILITY OF HIGH POWER LASER WINDOW MATERIALS	5. TYPE OF REPORT & PERIOD COVERED: Scientific - Interim
	6. PERFORMING ORG. REPORT NUMBER: Semiannual Tech Rpt No. 2
7. AUTHOR(s): Jacob L. Zar	8. CONTRACT OR GRANT NUMBER(s): F19628-75-C-0066
9. PERFORMING ORGANIZATION NAME AND ADDRESS: Avco Everett Research Laboratory, Inc. 2385 Revere Beach Parkway Everett, Mass. 02149	10. PROGRAM ELEMENT, PROJECT, TASK AREA & WORK UNIT NUMBERS: 2806-n/a-n/a
11. CONTROLLING OFFICE NAME AND ADDRESS: Air Force Cambridge Research Laboratories Hanscom AFB, Massachusetts 01731 Contract Monitor: Rudolf Bradbury/OPL	12. REPORT DATE: 15 October 1975
	13. NUMBER OF PAGES: 39
14. MONITORING AGENCY NAME & ADDRESS (if different from Controlling Office)	15. SECURITY CLASS. (of this report): Unclassified
	15a. DECLASSIFICATION/DOWNGRADING SCHEDULE

16. DISTRIBUTION STATEMENT (of this Report)

Approved for Public Release; Distribution Unlimited

17. DISTRIBUTION STATEMENT (of the abstract entered in Block 20, if different from Report)

18. SUPPLEMENTARY NOTES

This research was supported by the Defense Advanced Research Projects Agency, ARPA Order No. 2806

19. KEY WORDS (Continue on reverse side if necessary and identify by block number)

Laser Window Testing
Diamond Absorption Coefficient
Type II Diamond Laser Windows
Diamond Window Holder
Edge Cooled Windows
Laser Window Heating
Laser Window Distortion

20. ABSTRACT (Continue on reverse side if necessary and identify by block number)

This report describes the completion of a laser window test facility. It has been used to test the optical distortion of diamond windows while transmitting focussed radiation form a 10.6 μm laser. The continuous power exceeded 18 kilowatts. The average intensity over the focal spot is estimated to be 2.5×10^6 watts/cm^2. The optical distortion produced in the windows was measured with an interferometer and found to be 1/2 visible light fringe or less.

DD FORM 1 JAN 73 1473 EDITION OF 1 NOV 65 IS OBSOLETE

Unclassified

SECURITY CLASSIFICATION OF THIS PAGE (When Data Entered)

Some of the other results described in this report are the calibration of the laser window test facility, the measurement of the 10.6 μm, CW beam intensity profile at various distances from the mirror focus, a description of the calorimeter used to measure power, a description of the holder used to position and cool diamond windows, and measurement of the absorption of two diamond plates that have been tested as windows.

In addition to the experimental work, we have reviewed the published theory of the distortion of laser windows subjected to heat and pressure. Discrepancies and deficiencies have been found in generally accepted work that substantially affects the prediction of window performance.

TABLE OF CONTENTS

LIST OF ILLUSTRATIONS

Preceding page blank

I. INTRODUCTION

The principle work to be described in this report is the completion of a laser window test facility. It has been used to test the optical distortion of diamond windows while transmitting focussed radiation form a 10.6 μm laser. The continuous power exceeded 18 kilowatts. The average intensity over the focal spot is estimated to be 2.5×10^6 watts/cm^2. The optical distortion produced in the windows was measured with an interferometer and found to be 1/2 visible light fringe or less.

Some of the other results described in this report are the calibration of the laser window test facility, the measurement of the 10.6 μm, c.w. beam intensity profile at various distances from the mirror focus, a description of the calorimeter used to measure power, a description of the holder used to position and cool diamond windows, measurement of the absorption of two diamond plates that have been tested as windows.

In addition to the experimental work, we have reviewed the published theory of the distortion of laser windows subjected to heat and pressure. Discrepancies and deficiencies have been found in generally accepted work that substantially affects the prediction of window performance. It is planned to write an improved theory by which estimates may be made of the far field intensity that is achievable when a crystaline window is used to transmit large amounts of laser power.

II. DESCRIPTION OF THE LASER WINDOW TEST FACILITY

A facility has been constructed to test windows for absorption and optical distortion while transmitting a laser beam. The apparatus may be transported to any of the lasers, pulsed or continuous, available at this laboratory. However, the tests that are described in this report were done with the HPL® industrial laser. This is a closed cycle cw CO_2 electric laser

---

® Reg. U.S. Pat. Off.

Preceding page blank

deliver a continuous beam of 10.6 μm radiation of about 15 kilowatts. The laser is convenient to use. Controls may be set for the desired laser power, the run time, and the rate of rise and fall of power at the start and end of the run. There is a closed loop control system that maintains the power within 3 percent of the set power over long time periods.

Figure 1 is a photograph showing a diamond window located at a laser beam focus. Figure 2 is a schematic diagram of this experiment. The laser beam is transmitted to the test station as a collimated beam with a diameter of 3.8 cm. It is received by a plane mirror above the apparatus, reflected to a second plane mirror and then focussed by a concave mirror with an 81 cm focal length. Windows to be tested may be placed at any point in the laser beam where the diameter and intensity are appropriate. The illustrations show a diamond mounted in the holder.

To observe the window distortion, a diagnostic laser beam and an interferometer are provided. The second beam originates in a 3 mw helium neon laser. It first passes through a beam expander lens so that the window is completely illuminated. The interferometer is a Mach-Zehnder configuration, illustrated in Figure 2. This compares the optical path length of the beam passing through the window with a similar beam that bypasses it. Interference fringes are photographed during and after the transmission of the high power laser beam and are superimposed to show the extent of window distortion. With fast Polaroid film in the camera, the exposure time was 1/60 to 1/100 seconds, fast enough to preclude vibration or motion of the image during exposure.

The visible laser beam and the high power laser beam each make an angle of 20 degrees with the window surface. After passing through the window the high power laser beam is absorbed either on a calorimeter or in a beam dump. A ventilating system is provided so that vapor from the beam dump or from the window may be removed if any is expected to be generated. Compressed filtered nitrogen or helium is used to flush over the surface of windows for cooling or for removing dust particles.

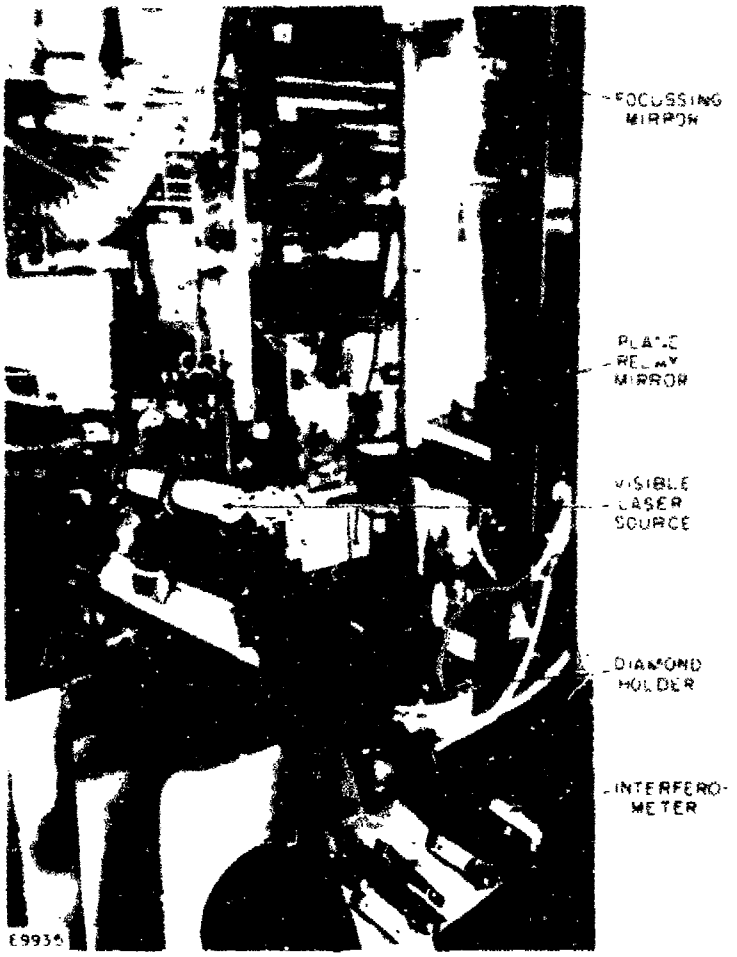

Fig. 1 Window Test Facility with Edge Cooled Diamond Window Holder

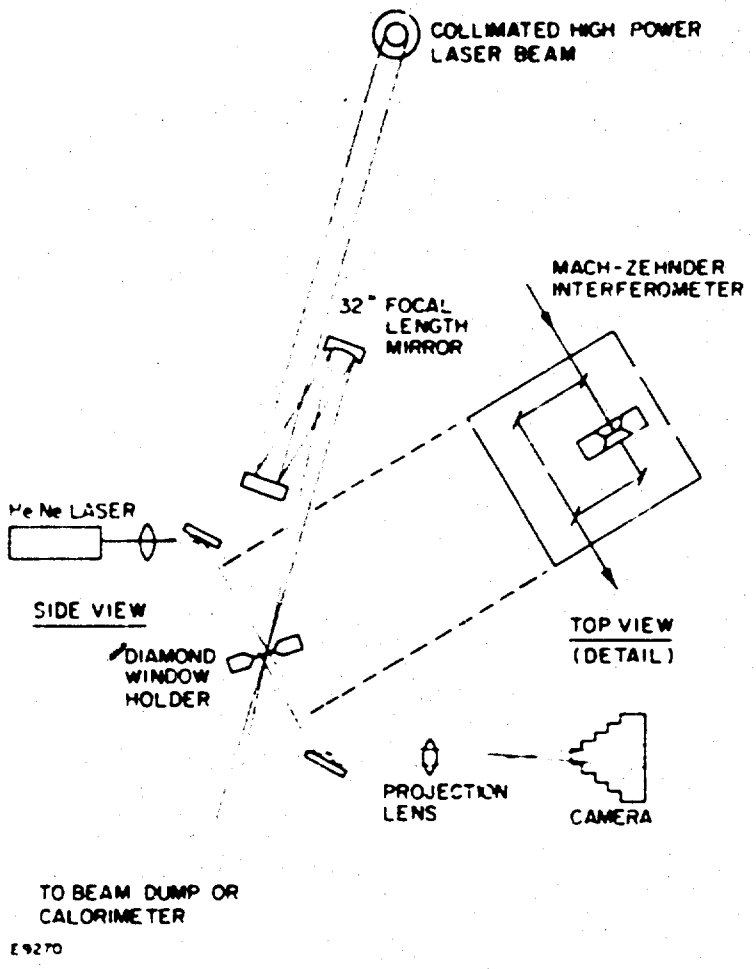

Fig. 2 Schematic of Laser Window Test Facility

As a preliminary to the test on solid windows, a number of calibrations were made to determine the beam characteristics at several locations between the focussing mirror and the focus. This was done by passing the laser beam through apertures of different size in a polished copper plate and then to a calorimeter. This calorimeter will be more completely described below, however, it has an anodized aluminum surface which is almost 100% absorbing at 10.6 μm.[2] The experimental arrangement is shown in Figure 3. Table I list the aperture diameter, the distance from the focus, the laser power setting, the laser time setting, and the energy received by the calorimeter during a calibration test. A preliminary burn pattern showed that the partially focused laser beam had an intensity profile that resembled a Gaussian. Therefore, this type of distribution was tested against the data to see how well it would fit.

$$I(r) = (P_o/\pi r_o^2) \exp(-r^2/r^2{}_o) \qquad (1)$$

where r_o determines the spreading of the beam and P_o is the power. The power transmitted through a hole is

$$P_h = \int_0^{r_h} 2\pi I(r)\, dr = P_o \left[1 - \exp(-r^2{}_h/r_o{}^2)\right] \qquad (2)$$

The constants P_o and r_o were determined by a least squares calculation using the actual data. The fitted curves thus obtained are shown plotted as the solid lines in Figure 4 with the actual data superimposed. In particular, the calculated value of P_o could be independently compared to the known power of the laser beam. In two cases, the difference was unmeasurable and in the third case, it was about 6% and is believed to result from an experimental misalignment rather than from any inherent property of the laser beam. Figure 5 shows the beam profiles obtained from the fitted Gaussian distribution. Figure 6 is a plot of r_o vs. the distance from the focus. The individual data points are shown as well as a straight line fitted to the data by a least squares curve fitting program.

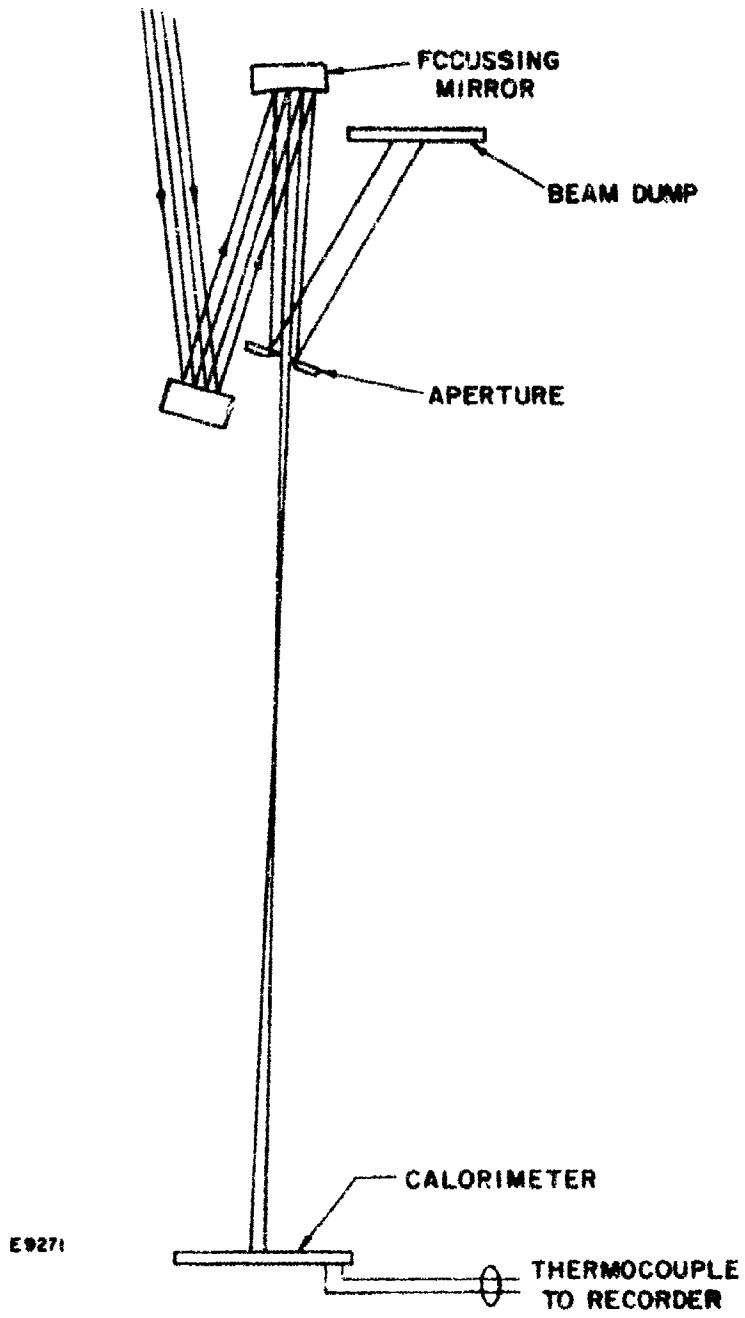

Fig. 3 Experimental Arrangement for Calibrating Window Test Facility Beam Distribution.

TABLE I

CALIBRATION OF 10.6 μm C. W. LASER WINDOW FACILITY

Run #	Aperture diameter cm	Distance from focus cm	Laser Power kW	Exposure Time sec	Calorimeter Energy Joules
15-3	2.14	27.9	2.05	.38	1250
15-4	2.14	27.9	2.05	.87	2180
15-5	2.14	27.9	2.00	1.86	4790
15-6	2.14	27.9	2.05	3.84	9610
15-7	1.270	27.9	2.05	1.87	3420
15-8	.871	27.9	2.10	1.87	2120
15-9	.638	27.9	2.00	1.88	1290
15-10	.638	27.9	2.05	1.88	1280
15-11	.411	27.9	2.05	1.86	504
15-12	.277	27.9	2.05	1.87	197
15-13	.638	27.9	4.1	1.91	2265
15-14	.638	27.9	8.05	1.91	3620
15-15	.638	27.9	12.05	1.96	4870
16-1	.277	5.08	2.05	1.87	86
16-2	.411	5.08	2.00	1.87	170
16-3	.638	5.08	2.05	1.85	360
16-4	.871	5.08	2.05	1.86	618
16-5	1.270	5.08	2.05	1.88	1310
16-6	2.14	5.08	2.10	1.88	2980
16-7	2.14	5.08	2.00	1.86	3040
16-8	8	5.08	2.05	1.85	5190
17-1	.158	12.2	2.10	1.85	291
17-2	.203	12.2	2.05	1.86	602
17-3	.241	12.2	2.00	1.86	892
17-4	.318	12.2	2.00	1.86	1490
17-5	.480	12.2	2.10	1.86	2718
17-6	.714	12.2	2.00	1.86	4148
17-7	.871	12.2	2.00	1.87	4670

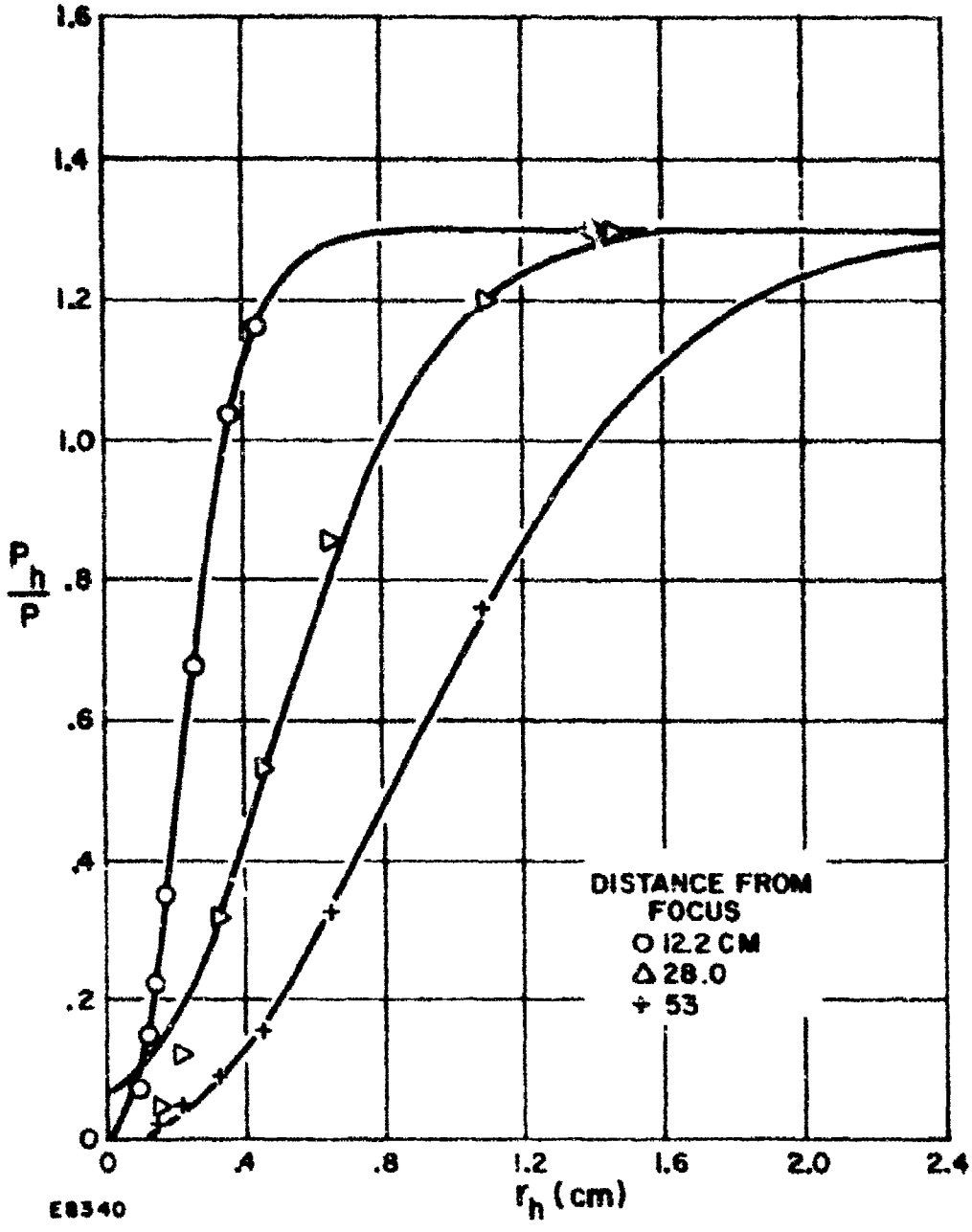

Fig. 4 Intensity of Laser Beam Transmitted through Apertures of Radius r_h

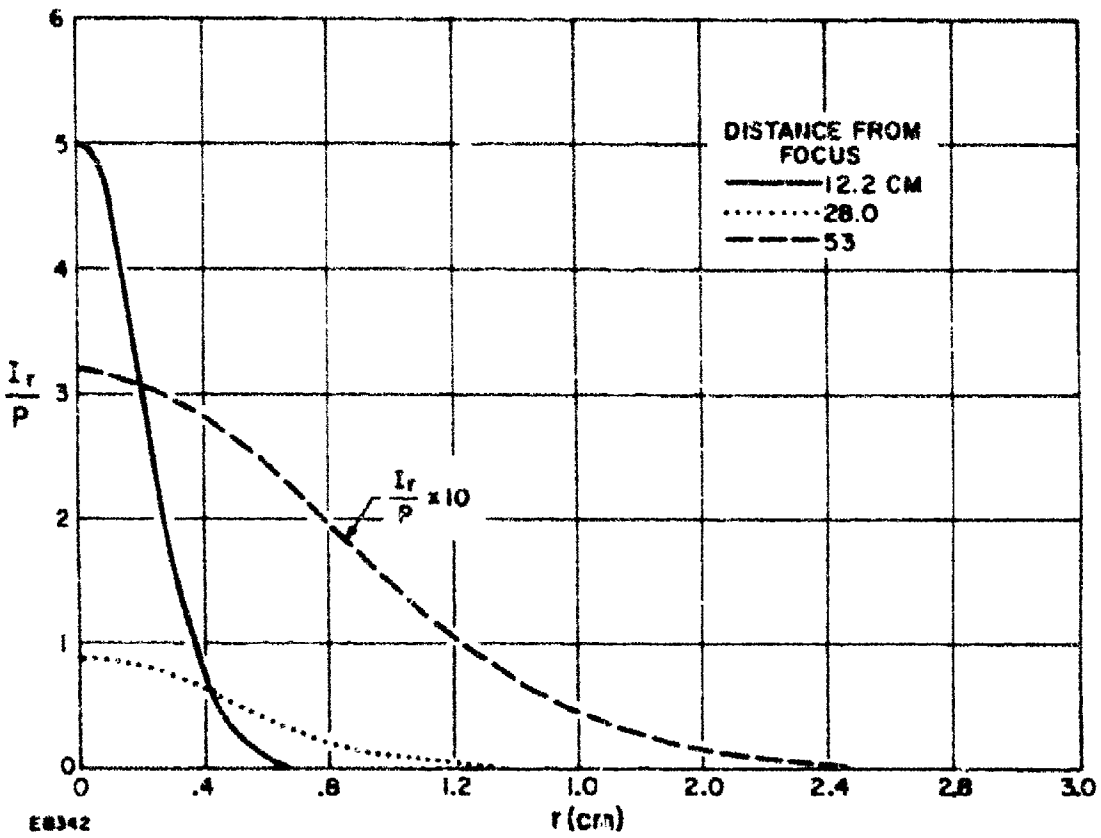

Fig. 5 Gaussian Beam Profile at Various Distances from Focus.

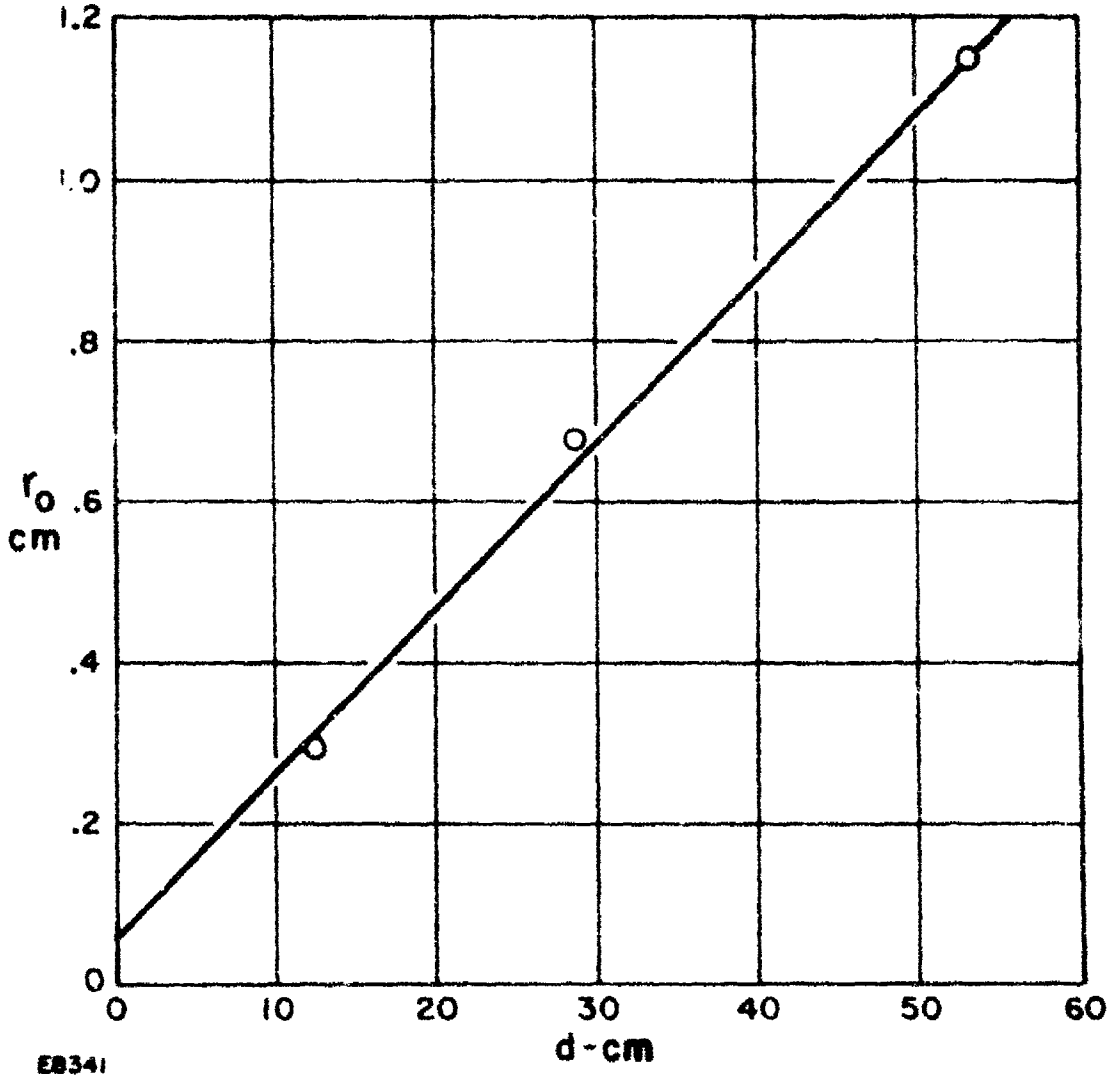

Fig. 6 Half Width to the 1/e Intensity for Laser Beams at Various Distances from Focus.

This curve is convenient for determining where to place windows with respect to the mirror focus.

The beam diameter at the focus was measured by making burns on a blackened steel plate located at the focus of the apparatus shown in Figure 2. The burn diameter was 1 mm and is correctly predicted in Figure 6. The 1 mm diameter is approximately the size of the focal spot that is theoretically predicted for the type of laser cavity used in the HPL laser combined with the type of optical system used in this test. For a beam power of 15 kw, the intensity averaged over the focal spot is 2×10^6 W/cm^2. The peak intensity is somewhat higher and it may be further increased by using mirrors of shorter focal length.

The calorimeter is shown in Figure 7. It was calibrated against laboratory standards. The energy absorber is a plate of #1100 aluminum alloy, 17.8 cm by 17.8 cm by .32 cm thick. The surface is anoidized. Our experience with this type of surface is that it absorbs .995 of the radiation at 10.6 μm.[2] The temperature rise of the absorber is measured with a thermopile consisting of 12 copper-constantan thermocouples running from the back of the absorber plate to an aluminum reference plate mounted 2" behind. The junctions are arranged on 2" centers and average the temperature of the entire plate. The reference junction temperature corresponds to the average room temperature in the vicinity of the calorimeter at the start of a test.

The specific heat for the calorimeter plate was corrected for the ratio of the density to that of pure aluminum. The measured density was 2.707 g/cm^3 whereas the density of pure aluminum is 2.702 g/cm^3. Therefore, the standard specific heat equation is multiplied by 2.702/2.707.

$$C_p = .869 + .00139T - 6.74 \times 10^{-6} T^2 \text{ Joule/g K} \qquad (3)$$

The thermocouple wires were calibrated against a precision thermometer with an emergent stem correction applied to the thermometer reading. The EMF obtained in this calibration was 41.45 μV/deg over the temperature range 20 to 40 deg C. This compares with the ANSI response for copper-

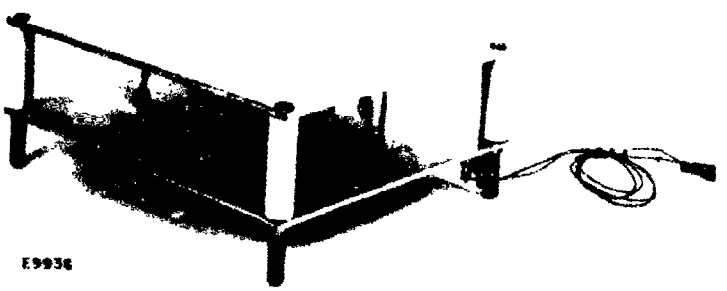

Fig. 7 Calorimeter Used in Laser Window Test Facility

constantan thermocouples which is 41.10 μV/deg over the same temperature interval. This agreement is consistent with the variability of different lots of thermocouple material. We believe that the thermocouple calibration represents the largest single systematic error in the calibration.

The calibration of the calorimeter is

$$J = .410 \times 10^5 V - 2.89 \times 10^5 V^2 - 9.42 \times 10^5 V^3 \qquad (4)$$

J is the absorbed energy in joules and V is the voltage of a 12 junction thermopile in volts. This calibration assumes a reference plate temperature in the vicinity of 20°C. The measuring circuit including the microvoltmeter should be wired with copper.

In order to use the calorimeter, it is brought to approximately room temperature by blowing air over the surface. Laser energy is allowed to fall on the surface for several seconds. The intensity must first be checked to insure that the surface of the absorber does not melt, and that the local temperature does not rise much above 100°C. A sensitive recorder is used for the output voltage. Particular attention is paid to the cooling curve after the laser has been turned off. This curve is extrapolated back to the midpoint between the laser start and stop time. By this means, the peak thermocouple voltage is approximately corrected for convection cooling of the absorber plate. This correction is small if the cooling curve has a much lower slope than the heating curve. Cooling by radiation is negligible because of the small amount of heating of the absorber. It is estimated that the calorimeter calibration is correct to better than 95%.

III. DIAMOND SAMPLE HOLDER

The C. W. power transmitted through a laser window depends as much on the efficiency of window cooling as on the absorption of the window material.

In a previous report of this project, we have concluded that diamonds may be selected by a spectroscopic test to have a value of the absorption coefficient, β less than .5 cm^{-1}.[3] In the experiments to be described, we have been able to select diamonds with β very much less than this.

A water cooled window holder in the shape of a radial nozzle has been designed in which the diamond is clamped at the edges of its parallel faces between two water cooled copper discs. This is shown in Figure 8. Thin annular gold washers distribute the force uniformly over the window surface. Water flowing at high velocity is brought into direct contact with the edge of the diamond. The surface heat transfer coefficient of the edge of the window is estimated by the following calculation. See Figure 9 for the notation.

Water enters the diamond holder at low velocity. In accordance with Bernoulli's equation, the coolant pressure drop is approximately $\Delta P = 1/2\, \rho V_1^2$ where V_1 is the velocity in the nozzle at the edge of the diamond. This is related to the mass flow

$$V_1 = \dot{M}/\pi\rho\,(r_2^2 - r_1^2) \tag{5}$$

The surface heat transfer coefficient, h, is given by a Colburn equation

$$h = .023\, k_b\, N_{Re}^{0.8}\, N_{Pr}^{0.4}/4r_h \tag{6}$$

where

r_h is the hydraulic radius of the duct, N_{Re} is the Reynolds number, N_{Pr} is the Prandtl number and k_b is the thermal conductivity of the cooling fluid.

By using the numerical values for water, $r_h = 1/2\,(r_2 - r_1)$ and

$$N_{Re} = 4\, V_1 \rho r_h/\mu = 2\,\dot{M}/[\,\pi\,\mu(r_2 - r_1)\,] \tag{7}$$

we obtain a simplified equation for the convective heat transfer to high velocity water

$$h = 6.75 \times 10^{-5}\, N_{Re}^{0.8}/r_h \quad W/cm^2\,K \tag{8}$$

by introducing equation (5), we obtain the surface heat transfer coefficient for this type of diamond holder

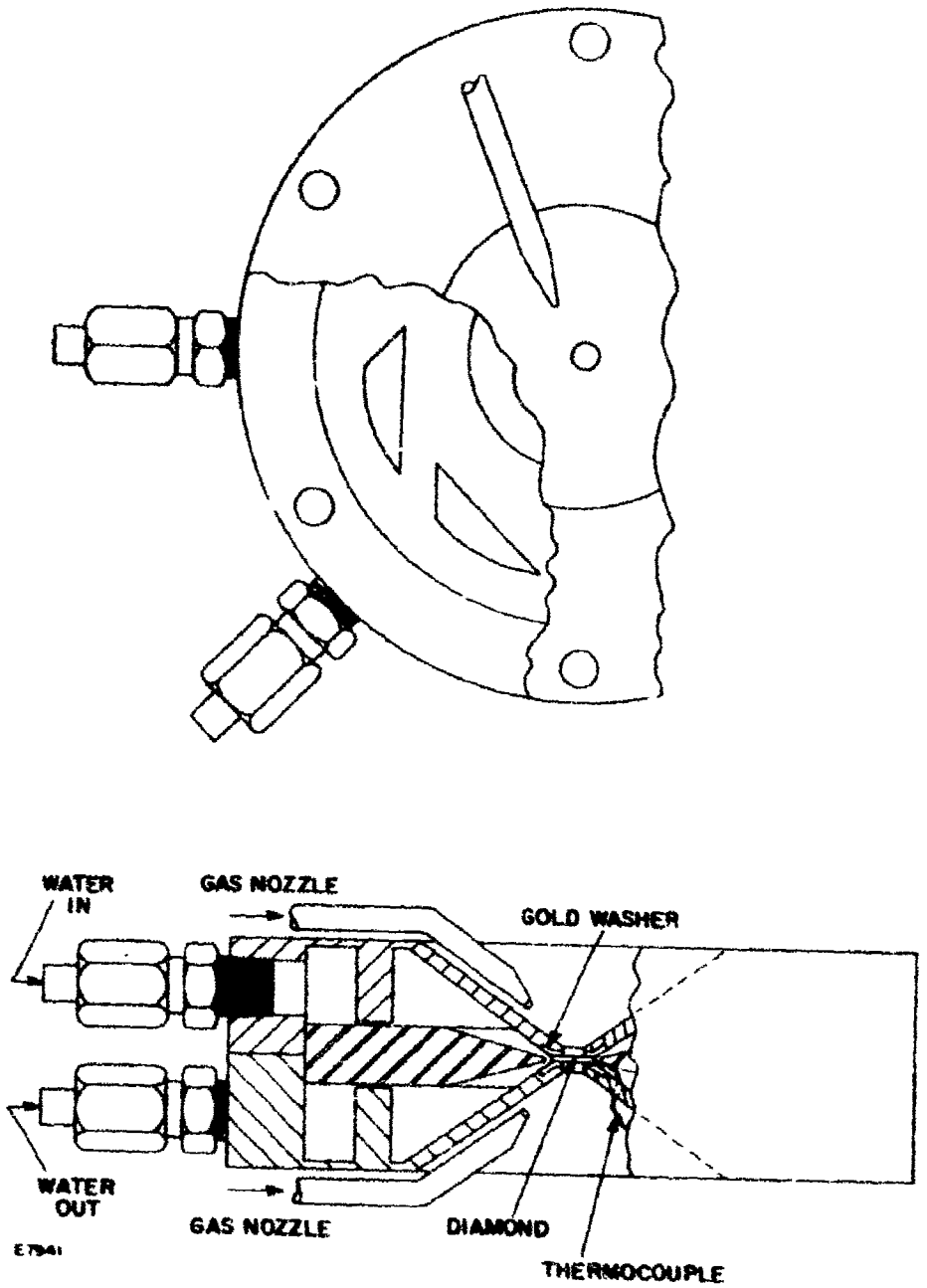

Fig. 8 Water-Cooled Diamond Window and Window Holder.

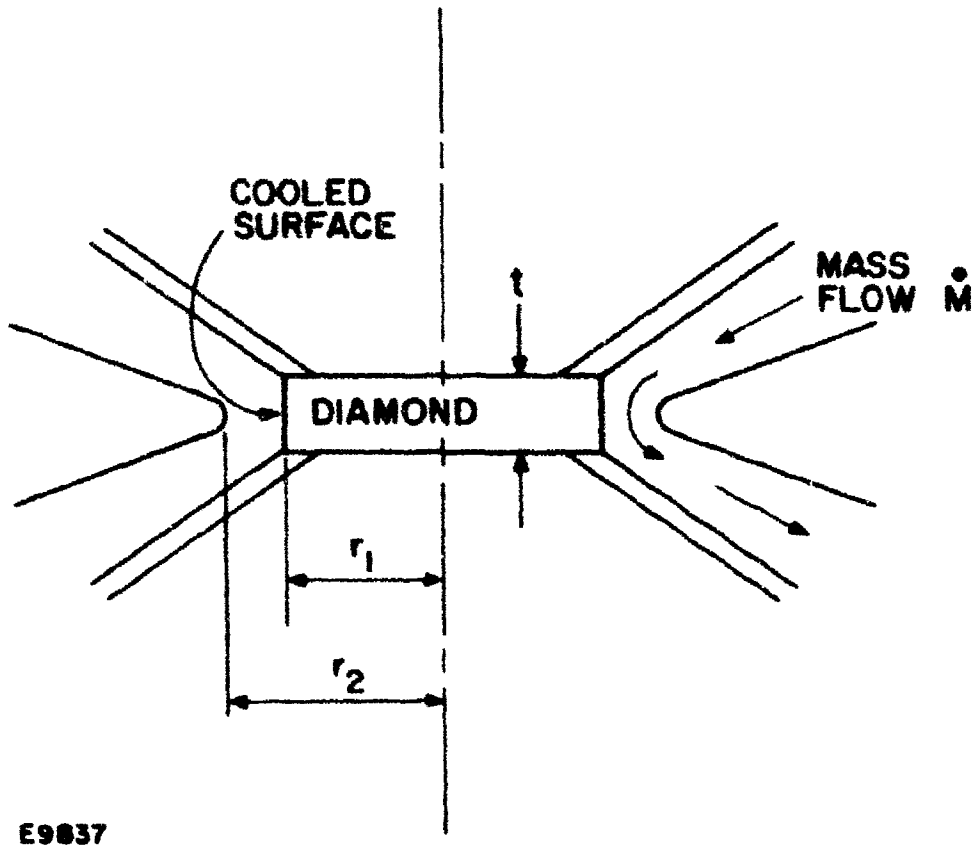

Fig. 9 Notation for Calculation of Heat Transfer Coefficient.

$$h = 3.10 \times 10^{-4} \quad \frac{\rho^{0.4} \Delta p^{0.4}}{\mu^{0.8} (r_2 - r_1)^{0.2}} \qquad (9)$$

The value of h is seen to be very insensitive to the clearance between the nozzle and the diamond and is only a weak function of the pressure drop. For a pressure drop of 20 psi (1.38×10^6 d/cm^2) and a radial clearance of .05 cm, the surface heat transfer is 7.7 W/cm^2 K, and the mass flow is 183 g/sec (less than 3 gallons per minute). In the diamond test experiments to be described, the pressure drop across the diamond holder was 7 psi and the calculated value of surface heat transfer coefficient was 5.0 W/cm^2 K. Table II list the significant physical properties of diamonds.

TABLE II

PROPERTIES OF NATURAL DIAMONDS

Density	$\rho = 3.52$ g/cc
Volumetric Heat Capacity	$\rho c = 1.8$ j/cc K
Elastic Modulus	$C_{11} = 9.5 \times 10^{12}$ d/cm^2
Linear Thermal Expansion	$\alpha = 1.2 \times 10^{-6}$ K^{-1} at 27° C
Thermal Conductivity for Type IIa[5]	k = 20 W/cm K at 30° C
Refractive Index	n = 2.39
Temperature Dependence[6]	$dn/dT = 1.9 \times 10^{-5}$ K^{-1}
Brewster Angle	$\theta = 67.$ deg
Absorption	$\epsilon = .01$ to $.3$ cm^{-1} for Type IIa
Tensile Strength	$F = 1.8 \times 10^{10}$ d/cm^2
Thermal Diffusivity	$k/\rho C = 11.$ cm^2/sec

As a result of the passage of laser radiation through the diamond, there will be an overall change in temperature and also a non-uniform temperature distribution centered about the region of peak flux. The change in transmitted wave phase front which is uniform transversely does not affect the far field intensity of a focussed laser beam and is unimportant for our present considerations. Non-uniform phase changes result from gradients in temperature or from thermoelastic stress. The present experiment is designed to show changes in transmitted phase front that result from non-uniform changes in thickness and changes in the index of refraction resulting from temperature gradients. The measurements are done with He-Ne radiation of .63 μm and the observed phase changes are more sensitive to heating than the phase of the 10.6 μm laser beam by the ratio $10.6/0.63 = 17$.

The heat absorbed by the diamond $q = \beta t P$ where P is the transmitted power, t is the diamond thickness, and β is the absorption. The change in temperature of an edge cooled diamond is determined by surface heat transfer at the cooled edge and by temperature gradients in the vicinity of the irradiated spot. The temperature rise of the cooled edge ΔT_2 is given by

$$\Delta T_2 = \beta P/2\pi r_1 h \qquad (10)$$

There is an additional temperature rise ΔT_1 due to the radial heat flow from a ro r_1 given by

$$\Delta T_1 = \beta P \ln (r_1/a)/(2\pi k) \qquad (11)$$

where a is the radius of the laser beam, assumed smaller than r.

The heating of the diamond by ΔT_2 produces no wave front distortion. In the region of ΔT_1, there is an expansion given by $\Delta t = \alpha t \Delta T_1$ where α is the expansion coefficient. In addition, there is a change in index of refraction $\Delta n = (dn/dT) \Delta T$. The number of waves of electromagnetic radiation in the window with a vacuum wave length λ along the optical path

Best Available Copy

is $N = tn/\lambda$. The relative phase of the wave will be $\phi = 2\pi N$ after transversing the plate. The change in phase with temperature is given

$$\frac{d\phi}{dT} = \frac{\partial\phi}{\partial n}\frac{dn}{dT} + \frac{\partial\phi}{\partial t}\frac{dt}{dT} \tag{12}$$

$$= (2\pi t/\lambda)\,[dn/dT + \alpha n] \tag{13}$$

Using the values for diamond listed in Table II we find that the phase change due to a change in index is 6.6 times as large as that due to a change in thickness.

IV. TESTS OF DIAMOND WINDOWS

A number of Type IIa natural diamond stones were inspected and three were selected to be cut into windows. As of the time of this report, two have been tested, the third has been received but has not yet been tested. These diamonds and the windows cut from them were designated by the diamond cutter as #800, and #SR13-1. The selection was made on the basis of the infrared spectrum of the uncut stones. Figure 10 is a portion of the spectra from 5 to 15 μm. Neither of these showed a noticeable dip in the vicinity of 7.5 μm and thus the stones were confirmed to be Type IIa diamonds. They were ordered cut with a slight wedge angle to be sure that they would not be received sufficiently parallel to have average transmission properties at 10.6 μm that are sensitive functions of the window thickness. The appearance of the diamonds was judged to be clear, colorless, and free from defects that could be ascertained with a 4X magnifying glass except at the extreme edges of the windows. The surface was smooth but no special polish was given other than the normal gem finish.[7] Table III gives the physical properties of the two windows.

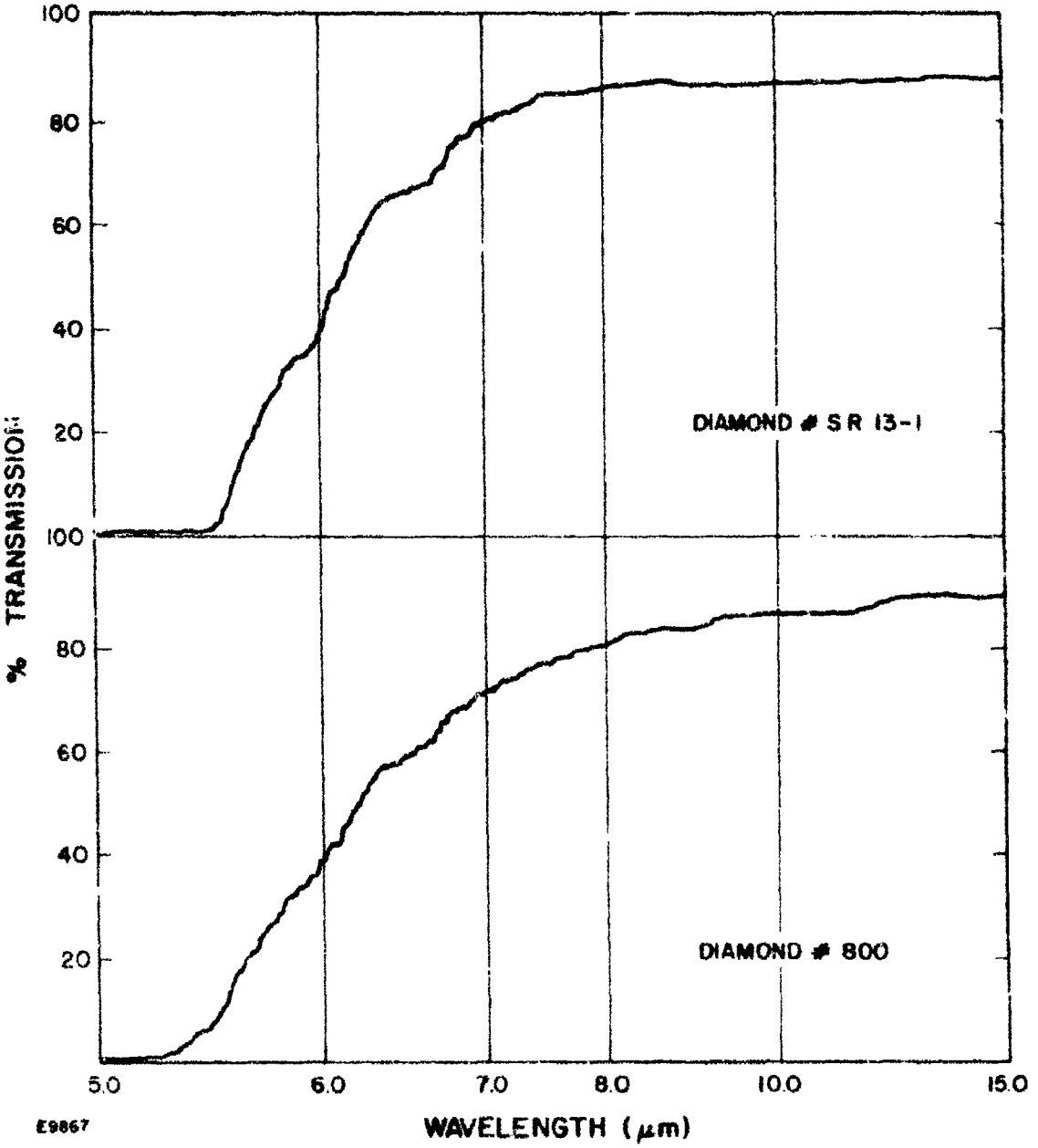

Fig. 10 Infrared Absorption Spectra of Diamond Window Stones.

TABLE III

DIAMOND WINDOW DESCRIPTION

	#800	#SR13-1
Diameter (cm)	.70	.57
Thickness (cm)(mean)	.0135	.224
Weight (g)	.1776	.0984
Wedge Angle (deg)	.38	.15

They were fitted into the water cooled diamond holder using a thin (.005 inch thick) gold annular washer to distribute the clamping forces over the surface. The diamond holder was carefully shimmed so that when tested with 60 psi air pressure, there was no leakage at the edge of the diamond through the clamp. A small leak at this point would have been unimportant because the diamond surface was continually flushed with nitrogen gas during the exposure and any slight trace of water (of which there was none) would have evaporated and been blown away. The clear aperture at the center of the window disc was 0.4 cm.

A tiny thermocouple was placed on the diamond and compressed between the gold washer and the face of the diamond. This thermocouple was constructed of 4 mil copper and constantan wires flattened at the tip to be very thin. Gold and copper have very nearly the same thermoelectric voltage against constantan. The hot junction was placed between the gold washer and the diamond face. The cold junction was 2 cm away and was at the temperature of the cooling water. Copper wires completed the circuit to the microvoltmeter. The gold washer on the side of the holder which contained the thermocouple was insulated from the body of the holder by a thin Teflon washer. The cold junction was also insulated. Thus a short circuit in the thermocouple wiring could be detected if present. It is very likely that the hot junction temperature was somewhat less than the diamond temperature. However, the behavior of the thermocouple, its instant response

and the rather close agreement between the measured and calculated diamond temperature lead us to the belief that the temperature measurements were indicative of the bulk temperature of the diamond itself.

The holder, including diamond were placed in the interferometer and adjusted so that the laser beam passed through the diamond at its focus (1 mm spot size). A second beam from a He-Ne laser passed through the diamond and was analyzed by the interferometer. Interference pictures were taken during the exposure and soon afterwards for comparison. The interferometer was steady and the pictures were reproducible. Laser power and running time was recorded. Another recorder showed the thermocouple voltage. Sucessive runs were taken with increasing power starting from 1 kilowatt up to the maximum that the laser would supply. Most of the runs were for 10 seconds. The thermocouple temperature began to rise as soon as the laser was turned on and reached a peak at 0.1 second. This is the approximate time for the laser to reach full power. At the very highest power levels, the ramp up time of the laser was adjusted to 0.5 seconds in order to avoid tripping of the overload circuits by power transients. At this time, the thermocouple response also agreed with the ramp up time. Approximately 0.1 seconds after the peak, the thermocouple voltage dropped from its peak value by a variable amount from 20% to 50% depending upon the particular run, however, this did not result from a change in laser power. It is not clear what was the reason for the decrease. A drop was seen even at 3kW and is not believed to be associated with film boiling because of the low degree of temperature rise. It is perhaps related to the reestablishment of turbulent flow patterns around the edge of the heated diamond or to the outgassing of surface layers adjacent to the diamond. It is not likely to result from film boiling or cavitation for two reasons. We shall see that the temperature rise that was recorded was too low to cause film boiling even at the maximum laser power. Secondly in this type of window holder the centrifugal force of the water, as it turns sharply at the edge of the window, presses against the window. The calculated value of this centrifugal overpressure for high values of water velocity is 2.3 atmospheres and this results in an increase in burn out heat flux as well as a reduction in the likelihood of cavitation.

The peak temperature rise was the one that was taken as the temperature of the diamond for the discussion that follows. This is because it was approximately proportional to the laser power, whereas the thermocouple reading after the temperature drop was not reproducible and in some cases erratic.

The laser beam reflected from the surface of the diamond was absorbed in a ceramic beam dump. The transmitted beam was allowed to fall into a second beam dump placed beneath the sample holder.

With diamond #800, we were able to achieve 20 kW output from the laser. The exposure time for this power was 5 seconds and an interferometer photograph was taken after 4 seconds. The thermocouple indicated a peak temperature rise of 36°C. Figure 11 shows the interferometer photograph taken while the 20 kW beam was passing through the window and Figure 12 is the interferometer picture taken a minute after the beam was turned off. Upon superposition of the two photographs, it can be seen that a fringe shift of about 1/2 visible light fringe has occurred in the central region of the diamond.

With diamond #SR13-1, the laser was not as well adjusted. The peak power reached was 18 kW. Figure 13 shows the interferometer photograph taken after 5 seconds of radiation. The interferometer photograph taken shortly after the laser was extinguished is shown in Figure 14. This diamond was not as flat as #800. The fringe curvature shown in the photograph indicates that cylindrical lensing is present in the diamond. Nethertheless, a superposition of the two photographs shows a barely perceptible fringe change caused by the transmission of the radiation. The peak temperature recorded by the thermocouple was 37°C. Although the transmitted power was slightly lower than diamond #800, the temperature was slightly higher. This is probably because of the smaller cooled surface.

The absorption of the diamonds at 10.6 μm was measured with the apparatus shown in Figure 15. A portion of the laser beam was transmitted through an aperture and brought to a focus at the diamond. The diamond

E9933

Fig. 11 Distortion of Diamond #800 by Transmission of 20 kW Focussed Laser Beam.

E9931

Fig. 12 Distortion of Diamond #800 Shortly after Test of Fig. 10.

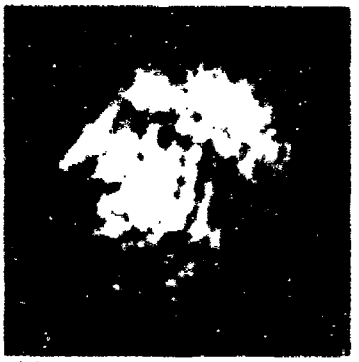

Fig. 13 Distortion of Diamond #SR13-1 by Transmission of 17 kW Focussed Laser Beam

Fig. 14 Distortion of Diamond #SR13-1 Shortly after Test of Fig. 12

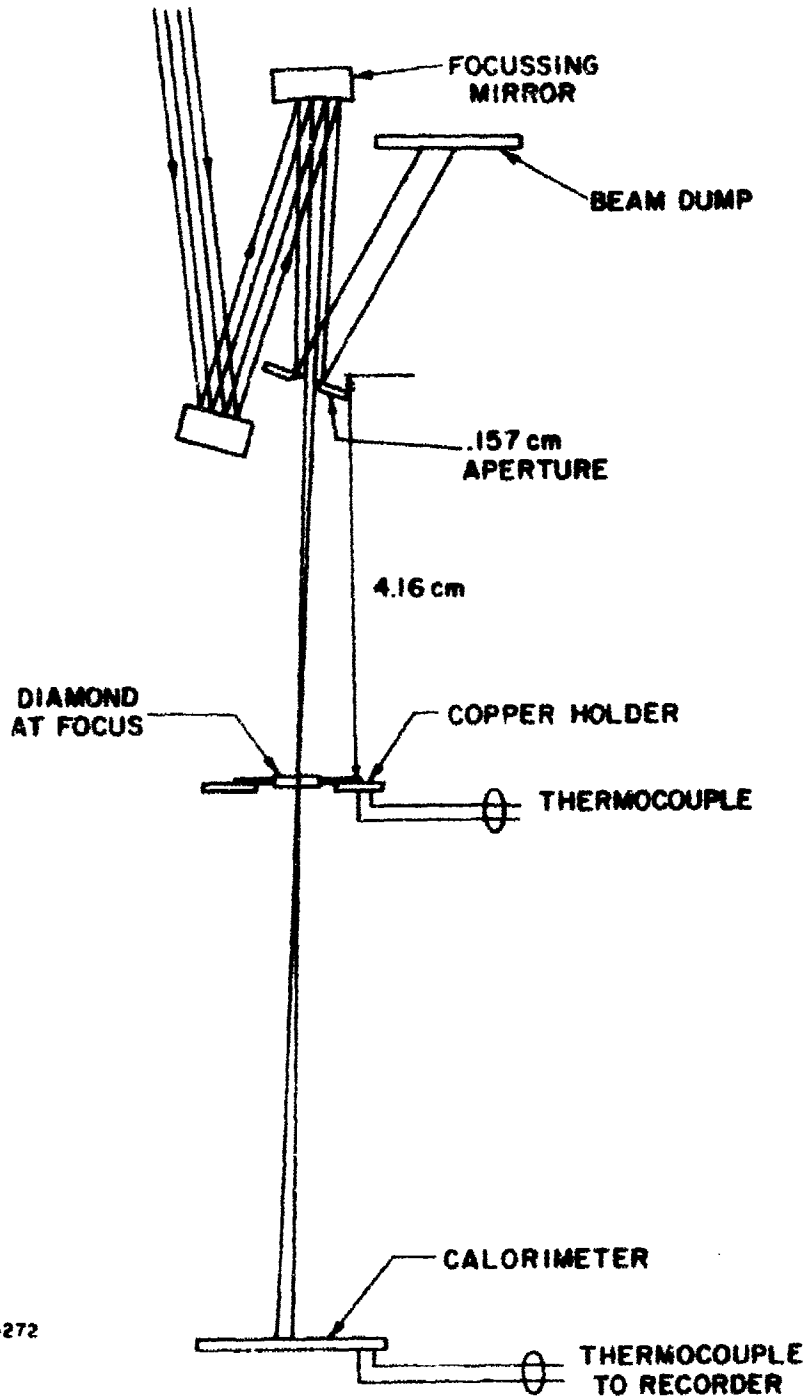

Fig. 15 Schematic of Apparatus Used to Measure the Absorption of Diamonds

was mounted in a small copper holder to which a thermocouple was attached. The transmitted radiation was measured with the calorimeter already described. The absorbed radiation was measured by the temperature rise of the diamond and its holder. After this measurement, the diamond was removed from the holder and the transmitted radiation measured by the same calorimeter. At this time, the radiation that was diffracted by the aperture and which struck the diamond holder was also determined. This energy was subtracted from the absorbed energy recorded for the diamond and holder together. Table IV gives the observed data.

TABLE IV

EXPERIMENTAL DATA FOR DIAMOND ABSORPTION TEST

	#800	#SR13-1
Exposure time (sec)	10.	10.
Mass of diamond (g)	.178	.098
Heat capacity of diamond (j/deg)	.0910	.0501
Mass of holder (g)	1.076	1.13
Heat capacity of holder (J/deg)	.419	.442
Incident power (w)	27.9	26.2
Absorbed power calorimeter + diamond (w)	.448	.637
Absorbed power calorimeter only (w)	.296	.520
Absorbed power - diamond only (w)	.151	.118
Diamond length (cm)	.135	.1125
Absorption (cm^{-1})	.040	.040

The calculation of the absorption from this data requires some analysis because of the high coefficient of reflection of diamond.

$$R = [(n_2 - n_1)/(n_2 + n_1)]^2 = .172 \qquad (14)$$

Here R is the reflected intensity from a single face of the diamond. By using a window cut with a small wedge we may average over all phases of the wave front. The energy entering the plate at the front surface is $I_1 = I_o (1-R)$ where I_o is the incident intensity outside of the plate. A portion of this intensity is reflected. This is $R_o = R I_o$. A portion of the energy transmitted by the plate is absorbed. This is given by

$$A_1 = I_1 [1 - \exp(-\beta t)] = I_o (1-R)[1 - \exp(-\beta t)] \qquad (15)$$

After passing through the plate, the intensity is reduced to the value

$$I_2 = I_1 \exp(-\beta t) = I_o (1-R) \exp(-\beta t) \qquad (16)$$

A portion of I_2 is reflected by the amount given in Equation 14 and the remainder is transmitted backwards through the plate. The reflected portion undergoes additional absorption on its return. Each successive pass of reflected radiation contributes additional absorption. Therefore, the total absorption is not just due to a single pass of radiation but is the sum of a series of terms of diminishing amplitude. The result of summing lead to a total absorbed energy

$$\mathbf{A} = A_1 + A_2 + A_3 + \ldots = I_o \frac{(1-R)[1-\exp(-\beta t)]}{1-R[\exp(-\beta t)]} \qquad (17)$$

For $\beta t \ll 1$. This reduces to

$$\mathbf{A} \approx I_o \beta t \qquad (18)$$

Note that **A** is independent of the reflection coefficient.

The total reflected energy can similarly be written

$$R = R_o + R_1 + \ldots = RI_o + I_o \frac{R(1-R)^2 \exp(-2\beta t)}{1-R^2 \exp(-2\beta t)} \quad (19)$$

For $\beta t \sim 1$. This reduces to

$$R = 2RI_o \quad (20)$$

which is independent of the absorption.
By substituting the data of Table IV into Equation 18 we find that the absorption for each diamond is .040.

In the first semiannual report, we reported on an examination of a group of 47 natural diamonds both Type I and Type II. Figure 5 of that report shows the lowest absorption that was found was .02 cm^{-1}. The second lowest diamond was .07 cm^{-1}. The remainder had larger absorption. The two diamonds that we have obtained for windows are close to the best that we have so far seen.

V. FUTURE PLANS

We have received samples of zinc selenide window material; both coated and uncoated. We have also recently received some potassium chloride crystals. We plan to test them in the window test facility using gas face cooling during the next reporting period.

In analyzing how test results on crystals would be interpreted and also in evaluating how large crystalline windows might be employed with powerful lasers, we have had occasion to examine some published work by others describing the effect of pressure and heating on windows aberation and on Strehl intensity. The published work has been extensively quoted in the literature and contributes to present day thinking on windows applications. We have reason to criticize past work from two standpoints. The first is conceptual. Formulae have been

used for the window deflection which give estimates of he expected deflections by considering the windows as thick plates. However, in windows, a more precise analysis must be employed because very slight errors in computing the optical path through a window will result in large errors in the phase of the transmitted radiation. Windows have many powers of 10 greater thickness than an optical wavelength. As a result we believe that the effect of the window distortion on far field intensity has been incorrectly evaluated.

The second source of error is mathematical. Errors have been made in the derivation of some equations. This had led to erroneous estimates for the far field intensity of a propagated light beam. These errors persist and are being included in new work. The fact that these errors exist and are significant has recently been confirmed to us by an independent consultant.

In view of the importance of crystalline laser windows, it seems appropriate to rethink and re-evaluate the effects of distortion and to prepare new maps showing which window materials may be used as a function of beam power, uniformity, and far field intensity. The new calculations should then be checked experimentally on a facility such as the Laser Window Test Facility at AERL. We are looking forward to discussions with our contract monitor on how we may assist in this reevaluation.

ACKNOWLEDGMENTS

The author wishes to thank G. W. Sutton, I. Itzkan, and D. Korff for discussion and advice on the problem of evaluating window distortion and far field intensity.

REFERENCES

1. Hoag, E., Pelase, H., Staal, S., and Zar, J. L., Performance Characteristics of a 10 kW Industrial CO_2 Laser System, Applied Optics, 13 1959, 1974.

2. Jacob, J., Pugh, E., Daugherty, J. and Northam, D., An Absolute Method of Measuring Energy Outputr from CO_2 Lasers. R.S.I., 44, 471 (1973).

3. Jacob L. Zar, AFCRL-TR-75-0264. Semiannual Technical Report No. 1, 15 April 1975.

4. Mc Adams, W. H., Heat Transmission, McGraw Hill Book Company, Inc. (1954).

5. Berman, R., Elect. Engineering (G. B). 42, 43, 1970.

6. International Critical Tables, McGraw Hill, Vol VII, p. 12 (1930).

7. Uncut stones and finished diamond plates were supplied by Lazare Kaplan and Sons, Inc., New York, N. Y. 10020.